Article

pubs.acs.org/Biomac

Polyplex Micelles with Double-Protective Compartments of Hydrophilic Shell and Thermoswitchable Palisade of Poly(oxazoline)-Based Block Copolymers for Promoted Gene Transfection

Shigehito Osawa,[†] Kensuke Osada,[*,‡,§] Shigehiro Hiki,[†] Anjaneyulu Dirisala,[†] Takehiko Ishii,[‡] and Kazunori Kataoka[*,†,‡,∥,⊥]

Departments of [†]Materials Engineering and [‡]Bioengineering, Graduate School of Engineering, The University of Tokyo, 7-3-1 Hongo, Bunkyo, Tokyo 113-8656, Japan

[∥]Division of Clinical Biotechnology, Center for Disease Biology and Integrative Medicine, Graduate School of Medicine, The University of Tokyo, 7-3-1 Hongo, Bunkyo, Tokyo 113-0033, Japan

[§]Japan Science and Technology Agency, PRESTO, Tokyo, Japan

[⊥]Innovation Center of NanoMedicine (iCONM), 3-25-14, Tonomachi, Kawasaki-ku, Kawasaki, 210-0821, Japan

Supporting Information

ABSTRACT: Improving the stability of polyplex micelles under physiological conditions is a critical issue for promoting gene transfection efficiencies. To this end, hydrophobic palisade was installed between the inner core of packaged plasmid DNA (pDNA) and the hydrophilic shell of polyplex micelles using a triblock copolymer consisting of hydrophilic poly(2-ethyl-2-oxazoline), thermoswitchable amphiphilic poly(2-*n*-propyl-2-oxazoline) (PnPrOx) and cationic poly(L-lysine). The two-step preparation procedure, mixing the triblock copolymer with pDNA below the lower critical solution temperature (LCST) of PnPrOx, followed by incubation above the LCST to form a hydrophobic palisade of the collapsed PnPrOx segment, induced the formation of spatially aligned hydrophilic−hydrophobic double-protected polyplex micelles. The prepared polyplex micelles exhibited significant tolerance against attacks from nuclease and polyanions compared to those without hydrophobic palisades, thereby promoting gene transfection. These results corroborated the utility of amphiphilic poly(oxazoline) as a molecular thermal switch to improve the stability of polyplex gene carriers relevant for physiological applications.

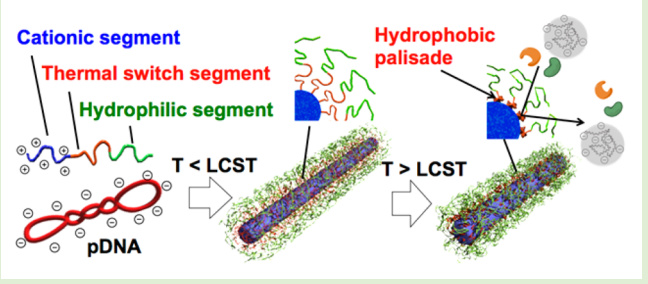

INTRODUCTION

Polyplex micelles prepared from plasmid DNA (pDNA) and block copolymers composed of hydrophilic and cationic segments are highly regarded as a competent delivery system for gene therapy.[1−7] The properties of the micelle are derived from its core−shell structures; the inner core serves to encapsulate pDNA through complexation with the cationic segment, and the outer shell formed from hydrophilic segment shields the core from the surrounding physiological environment.[1−7] In addition to these potent structural properties, the integration of functionalities to improve efficacy is in demand to promote the use of polyplex micelles in practical applications. To this end, the use of ABC-type triblock copolymers is appealing because the additional segment is capable of serving as a dedicated compartment to contain functionalities.[8−10] Additionally, ABC triblock copolymers enable spatial alignment of this compartment at specific positions in polyplex micelles by choosing an appropriate segment sequence in the block copolymer. Following this, polyplex micelles with layered structures containing an outer hydrophilic palisade, middle functional compartment, and inner core compartment for pDNA encapsulation could be formed from triblock copolymers containing a hydrophilic A segment, functional B segment, and cationic C segment.[8−10] These structures are distinguishable from polyplex micelles prepared from a conventional diblock copolymer system with functional moieties randomly conjugated to cationic segments.[11,12] Noteworthy, the potency of the triblock copolymer-mediated polyplex micelles has been verified in investigations that attempted to introduce endosome escape functionalities to the middle B segment by incorporating a segment retaining buffering capacity[8] or a segment encapsulating dendrimer phthalocyanine (DPc) as a photosensitizer that was then employed for photochemical internalization (PCI).[10]

Stimulating the pronounced potency of the triblock copolymers, we hereby propose to utilize the middle compart-

Received: October 29, 2015
Revised: December 13, 2015
Published: December 18, 2015

DOI: 10.1021/acs.biomac.5b01456
Biomacromolecules 2016, 17, 354−361

ment as a protective layer to address the critical issue of stability of micelles within physiological environments for the promotion of gene transfection. As factors that hamper the stability of polyplex micelles, nuclease attack of the DNA payload is considered serious as it directly impairs the transfection ability of polyplex micelles.[4,6] Furthermore, interactions with anionic glycosaminoglycans (GAGs),[13,14] such as chondroitin sulfate (CS) and heparan sulfate (HS) located in the cellular surface and extracellular matrix (ECM), are also a concern because they may cause dissociation of the polyplex micelles through a polyion exchange reaction,[11,15−17] eventually impeding the internalization of polyplex micelles into target cells. Therefore, protection of polyplex structures from these interfering substances is a critical issue for the micelles to function properly in harsh biological environments. The outer shell of the polyplex micelles consisting of hydrophilic segments do protect the polyplex core from these interfering substances; however this alone may not be sufficient for thoroughly circumventing this issue. In this regard, we attempted to prepare bulk hydrophobic palisades positioned at the middle compartment utilizing the intriguing "switchable" nature of a thermoresponsive polymer. To this end, a triblock copolymer consisting of poly(2-oxazoline)s (POxs), which have progressively been drawing attention as biomaterials,[18] was utilized. This copolymer consisted of poly(2-ethyl-2-oxazoline) (PEtOx) as the shell forming A segment due to its hydrophilicity and biocompatibility, which was approved by the U.S. Food and Drug Administration.[18] The B segment consisted of thermoresponsive poly(2-*n*-propyl-2-oxazoline) (PnPrOx) to generate the bulk palisade, which has a LCST below physiological temperature (30 °C).[19,20] The C segment consisted of a cationic polypeptide of poly(L-lysine) (PLys) to promote pDNA binding.[1,2,8,10] To take advantage of the thermoswitchable property of thermoresponsive PnPrOx of the designed PEtOx-*b*-PnPrOx-*b*-PLys triblock copolymer, a two-step preparation procedure was adopted; polyion complexation between pDNA and the triblock copolymers was conducted below the LCST of the middle segment to prepare the conventional core−shell polyplex micelles, and subsequently elevating the temperature to a physiological temperature, which was above the LCST, to cause the middle segment to become hydrophobic (Scheme 1). This procedure circumvented the potential occurrence of interpolymer association prior to

Scheme 1. Schematic Illustration of Polyplex Micelles with Spatially Regulated Hydrophilic−Hydrophobic Double-Protective Compartments Prepared from Triblock Copolymers with a Thermoresponsive Unit

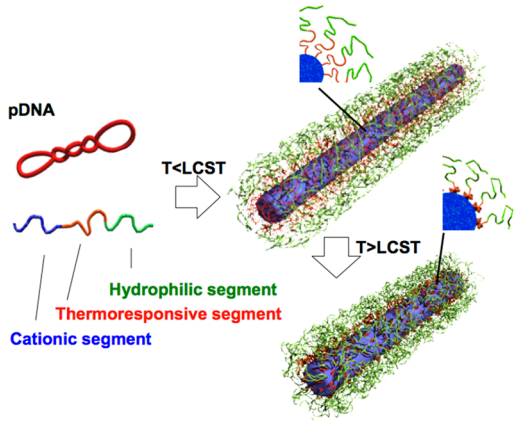

Scheme 2. Synthetic Scheme To Prepare Triblock Copolymer of PEtOx-*b*-PnPrOx-*b*-PLys

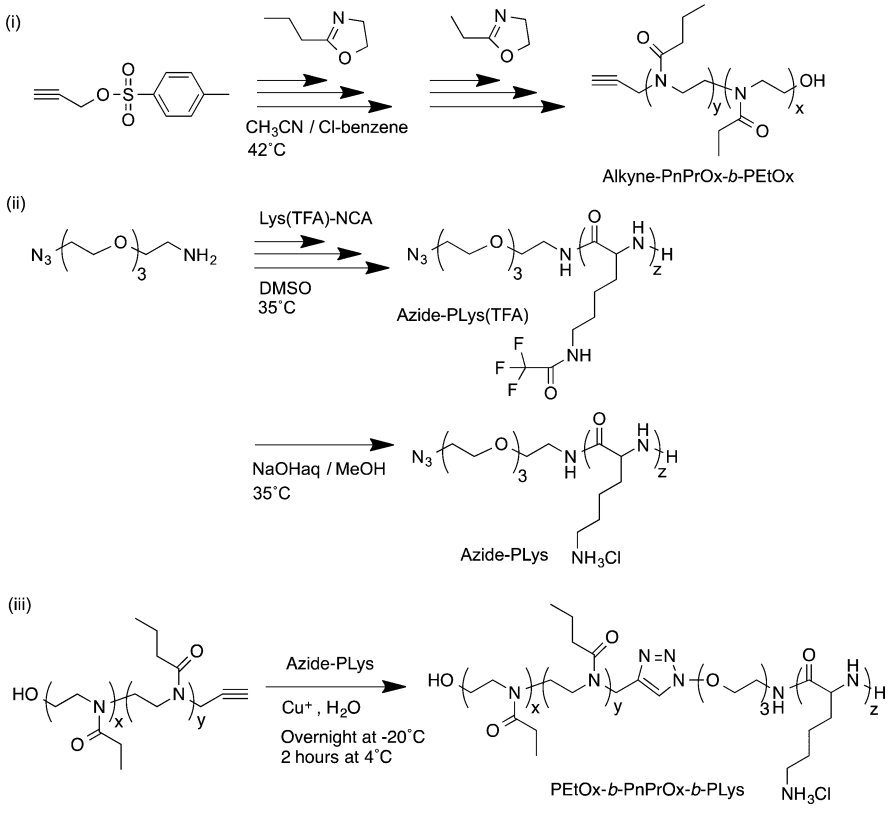

DOI: 10.1021/acs.biomac.5b01456
Biomacromolecules 2016, 17, 354−361

complexation with pDNA, which may proceed if an inherently hydrophobic unit is used instead of the amphiphilic thermoresponsive polymer, thereby assuring smooth polyion complexation to form well-compartmentalized polyplex micelles. Importantly, the fairly narrow molecular weight distribution of the POx adopted by the living cationic ring-opening polymerization[20] could also have contributed to the formation of stable compartmentalized structures because it facilitates smooth alignment of segment boundaries. The PLys segment was also prepared in a controlled manner using *N*-carboxyanhydride (NCA) ring-opening polymerization.[21] With this proposed POx-based triblock copolymer incorporating the conceptual molecular thermal switch properties, we investigated the formation of compartmentalized polyplex micelles to improve their stability and their transfection efficiencies in a physiological environment.

2. MATERIALS AND METHODS

2.1. Materials. *Nε*-Trifluoroacetyl-L-lysine *N*-carboxy anhydride (Lys(TFA)-NCA) was prepared using the Fuchs-Farthing method.[21] Acetonitrile (Wako Pure Chemical Industry, Osaka, Japan), 2-ethyl-2-oxazoline (EtOx; Tokyo Kasei Kogyo Co., Ltd., Tokyo, Japan), 2-*n*-propyl-2-oxazoline (nPrOx; Tokyo Kasei Kogyo Co., Ltd., Tokyo, Japan), and dimethyl sulfoxide (DMSO; Wako Pure Chemical Industry, Osaka, Japan) were used after distillation over calcium hydride. Propargyl *p*-toluenesulfonate (Tokyo Kasei Kogyo Co., Ltd., Tokyo, Japan) and chlorobenzene (Wako Pure Chemical Industry, Osaka, Japan) were used after distillation over phosphorus pentoxide. The 11-azido-3,6,9-trioxaundecan-1-amine (Sigma-Aldrich, St. Louis, MO) initiator was used as received. Luciferase-coded pDNA with a CAG promoter (pCAG-Luc2, 6477 bp) and human hepatoma cells (Huh7) were provided from the RIKEN BioResource Center (Tsukuba, Japan). The cell culture medium was prepared using 500 mL of Dulbecco's modified Eagle's medium (DMEM) (Sigma-Aldrich Co., Madison, WI) and 50 mL of fetal bovine serum (FBS) (Dainippon Sumitomo Parma Co., Ltd., Osaka, Japan). Dulbecco's phosphate-buffered saline (DPBS) and chondroitin sulfate A sodium salt from bovine trachea were purchased from Sigma-Aldrich Co. (Madison, WI). Recombinant DNase I was purchased from Takara Bio Inc. (Tokyo, Japan). Cy3-labeled pDNA was prepared using a Label IT Tracker Intracellular Nucleic Acid Localization Kit (Mirus Bio Corp., Madison, WI) according to the manufacturer's instructions. Hoechst 33342 and calcein were purchased from Dojindo Laboratories (Kumamoto, Japan). Cell culture lysis buffer was purchased from Promega Co. (Madison, WI).

2.2. Synthesis of Alkyne-Terminated Poly(2-ethyl-2-oxazoline)-Poly(2-*n*-propyl-2-oxazoline) (Scheme 2i). The oxazoline-based block copolymer with an alkyne functionality at the α-end (alkyne-PnPrOx-*b*-PEtOx) was synthesized by cationic ring opening polymerization of oxazolines[20,22] using the sequential monomer addition technique.[23] Briefly, 72.9 mg of propargyl *p*-toluenesulfonate was used as an initiator (0.347 mmol) and was dissolved in 9 mL of an acetonitrile/chlorobenzene mixture (50/50 vol %). Then, 2.77 g of nPrOx (24.5 mmol, 70.6 equiv mol to the initiator) was added to the mixture for polymerization. After 6 days of stirring at 42 °C under an argon atmosphere, the molecular weight (M_w) and the molecular weight distribution (M_w/M_n) of the product was measured using matrix-assisted laser desorption ionization-time-of-flight mass spectroscopy (MALDI-TOF-MS; Bruker ultrafleXtreme, Bruker Daltonics, Bremen, Germany) with 1,8,9-trihydroxyanthracen (THAT) as a matrix. The M_w and M_w/M_n values of the polymer were determined to be 8030 g/mol and 1.01, respectively. Subsequently, 3.47 g of the EtOx monomer (35.0 mmol, 101 equiv mol to the initiator) was added to the reaction solution and stirred at 42 °C for another 6 days under an argon atmosphere. The reaction was terminated by adding a mixture of 10 mL of methanol and 1 mL of 0.5 M NaOH(aq). The obtained solution was dialyzed against methanol three times and against deionized water three times using Spectra/Por molecular porous membrane tubing (MWCO 12000−14000; Spectrum Laboratories, Inc., Rancho Dominguez, CA). The dialyzed solution was then lyophilized to obtain a white powder (4.16 g, 0.23 mmol, 66.7% yield). The M_w of the final product was determined to be 17500 g/mol by MALDI-TOF-MS, demonstrating that the M_w of the PEtOx segment was 9470 g/mol. The product was also evaluated by ^{1}H NMR (400 MHz) (JEOL ECS-400, JEOL, Tokyo, Japan) recorded in D_2O at 15 °C (charts are provided in the Supporting Information, Figure S3a).

2.3. Synthesis of Azide-Terminated Poly(L-lysine) (Azide-PLys; Scheme 2ii). An initiator of 11-azido-3,6,9-trioxaundecan-1-amine (44 mg, 0.20 mmol) dissolved in 2 mL of DMSO was added to a solution of Lys(TFA)-NCA (2.22 g, 8.2 mmol) in 22 mL of DMSO. The solution was stirred for 48 h at 35 °C under an argon atmosphere for polymerization. DMSO was removed by dialysis against water followed by collection of the product, azide-PLys(TFA), which was obtained as a white powder by lyophilization (1.42 g, 76.8% yield). Then, 1.0 g of azide-PLys(TFA) was dissolved in 50 mL of methanol and mixed with 15 mL of a 1 M NaOH(aq) solution to deprotect the TFA groups. After 6 h of stirring at 35 °C, the solution was sequentially dialyzed against 0.01 M HCl and deionized water (MWCO 3500). The resulting azide-PLys was obtained as a white powder after lyophilization (632 mg, 90.0% yield). The obtained azide-PLys was characterized by aqueous phase size exclusion chromatography (SEC) using an AKTA explorer100 system equipped with a Superdex 200 prep grade column (GE Healthcare, Buckinghamshire, U.K.) at 8 °C using 10 mM acetate buffer (pH 4.6) containing 0.5 M NaCl. The effluent was monitored by a UV detector at 220 nm. The degree of polymerization (DP) of the Lys units of azide-PLys was determined to be 46 based on ^{1}H NMR analysis by comparing the peak areas of the α- (NHCOC$\underline{H}$NH, δ = 4.25−4.38 ppm), β-, γ-, and δ-methylene protons (-C$\underline{H}_2$C$\underline{H}_2$C$\underline{H}_2$CH$_2$NH$_3$, δ = 1.30−1.88 ppm) of the side chain of the Lys unit to the methylene protons of the α-end of the initiator, [11-azido-3,6,9-trioxaundecan-1-amine (N_3C$\underline{H}_2$C$\underline{H}_2$OC$\underline{H}_2$C$\underline{H}_2$OC$\underline{H}_2$C$\underline{H}_2$OC$\underline{H}_2$C$\underline{H}_2$NH, δ = 3.51−3.75 ppm); Figure S3b].

2.4. Synthesis of the Triblock Copolymer, PEtOx-*b*-PnPrOx-*b*-PLys (Et9-Pr8-L) (Scheme 2iii). A triblock copolymer was prepared using copper-catalyzed "Click Chemistry".[24] Azide-PLys (33 mg, 0.0044 mmol) and alkyne-PnPrOx-*b*-PEtOx (200 mg, 0.011 mmol) were separately dissolved in 1 mL of deionized water. Then, both solutions were mixed, and $CuSO_4{\cdot}5H_2O$ (2.8 mg, 0.011 mmol) and sodium ascorbate (2.2 mg, 0.011 mmol) were added as catalysts. To perform a freeze−thaw cycle to accelerate the "Click" reaction, the solution was frozen at −30 °C overnight and was thawed at 4 °C for 2 h.[25] Then, the sample was dialyzed against deionized water five times (MWCO 12000−14000) and lyophilized. The obtained powder sample was dispersed in 10 mL of acetone (poor solvent for PLys) and centrifuged to obtain the triblock copolymer as precipitates. After the supernatant was decanted, the precipitate was dispersed in acetone again and the same process was repeated three times. Then, the precipitate was dialyzed against deionized water three times (MWCO 12000−14000) and collected as a white powder after lyophilization. The final product was characterized by aqueous phase SEC under the same conditions as described above (Figure S2).

2.5. Synthesis of the Diblock Copolymer, PEtOx-*b*-PLys (Et10-L, Et18-L). The diblock copolymer of PEtOx-*b*-PLys was synthesized as a control block copolymer using the same procedure to prepare the triblock copolymer. Two PEtOx-alkyne blocks with different molecular weights (M_w = 10300 and 17700) were synthesized for conjugation with PLys (DP = 46) and were named Et10-L and Et18-L, respectively.

2.6. Preparation of Polyplex Micelles. The series of block copolymers and pDNA were separately dissolved in 10 mmol of HEPES buffer (pH 7.4) at 4 °C. The polyplex micelles were prepared by mixing 1-unit volume of the block copolymer solution to 2-unit volumes of the pDNA solution (50 μg/mL) at 4 °C. The residual molar ratio of the amino groups (N) in the PLys segment to the phosphate groups (P) in pDNA (N/P ratio) was 2. The polyplex

DOI: 10.1021/acs.biomac.5b01456
Biomacromolecules 2016, 17, 354−361

micelles were then incubated at 37 °C for 10 min to turn the PnPrOx segment into a collapsed state.

2.7. Dynamic Light Scattering (DLS) Measurements. The hydrodynamic diameter and polydispersity index (PDI) of the polyplex micelles were evaluated by DLS measurements using an Ar laser (λ = 532 nm) from a scattering angle of 173° (Zetasizer Nano-ZS, Malvern Instruments, Worcestershire, U.K.). The rate of decay in the photon correlation function was analyzed using the cumulant method and by applying the Stokes−Einstein equation to obtain a cumulant diameter for the polyplex micelles. The effect of temperature for the polyplex micelles of Et9-Pr8-L was investigated from 10 to 40 °C at 5 °C intervals with 30 min preincubation times at each temperature.

2.8. Determination of Thermoresponsivity of the Polyplex Micelles by ^{1}H NMR. The thermoresponsivity of PnPrOx within the polyplex micelles was investigated by ^{1}H NMR. The peak area derived from the methyl protons on a side chain of PnPrOx (δ = 0.83−0.98 ppm) and that of PEtOx (δ = 0.99−1.15 ppm) was measured and normalized against the peak area of 0.05% TMS dissolved in D_2O. The temperature was increased from 15 to 40 °C in a stepwise manner with 30 min incubation times before each measurement.

2.9. Transmission Electron Microscopy (TEM) Observations of Polyplex Micelle Structures. A TEM sample solution for observing the polyplex micelles was prepared by mixing 10 μL of a twice-diluted polyplex micelle solution with 10 μL of 2% uranyl acetate on ice. A TEM grid (Nisshin EM Co., Tokyo, Japan), which had been hydrophilized by an Eiko IB-3 ion coater (Eiko Engineering Co., Ltd., Shimane, Japan), was dipped into the sample solution for 30 s. The excess solution was blotted away. TEM sample preparation for the thermally treated polyplex micelles, which had been incubated at 37 °C for 10 min, was conducted on a 37 °C heater. The grids were observed by an H-7000 TEM (Hitachi Ltd., Tokyo, Japan) operated at an acceleration voltage of 75 kV. The lengths of the rod-shaped polyplex micelles were measured using ImageJ software (NIH, Bethesda, MD) to obtain rod length distributions.

2.10. Tolerance against DNase I. The polyplex micelle solutions (20 μL, 0.667 μg of pDNA) were incubated at 37 °C for 10 min and then mixed with 5 μL of DNase I solution (0.05 U/μL), 3 μL of 10 × DNase I buffer (Takara Bio Inc., Tokyo, Japan), and 2 μL of 10 mM HEPES buffer. After a 15 min incubation of the solution at 37 °C, 5 μL of 50 mM EDTA was added to each polyplex micelle solution to stop the reaction, which was further incubated at 80 °C for 2 min to inactivate DNase I. Then, 5 μL of a sodium dextran sulfate solution (5 mg/mL) was added to each solution and incubated at 4 °C for 2 h to dissociate the polyplex micelles. After incubation, 15 μL of each solution was loaded onto a 0.9 wt % agarose gel with 3 μL of the 6 × loading buffer, followed by electrophoresis at 100 V for 60 min. Migration of pDNA in the gel was visualized by soaking the gel in an EtBr solution (0.5 mg/L). Images were captured with an Epi-LightUV FA500 monochrome CCD camera imaging system (AISIN Taitec, Kosmos Kenkyo Inc., Tokyo, Japan).

2.11. Tolerance against CS. The polyplex micelle solutions were incubated with various concentrations of CS (16.7, 25.0, or 33.3 mg/mL) containing 10 mM HEPES buffer supplemented with 150 mM NaCl at 37 °C for 2 h. Aliquots of 15 μL of each mixture were then loaded onto a 0.9 wt % agarose gel with 3 μL of 6 × loading buffer. After electrophoresis at 100 V for 60 min, pDNA on the gel was visualized in the same manner as described above.

2.12. Cellular Uptake Study. Huh7 cells were seeded on 48-well culture plates (10000 cells/well) and incubated overnight in 200 μL of DMEM medium containing 10% FBS at 37 °C in a humidified atmosphere with 5% CO_2. After refreshing the medium, the cells were treated with polyplex micelle solutions prepared from Cy3-labeled pDNA (0.5 μg of pDNA/well) for 24 h. Then, 25 μL of calcein (3.3 μg/mL) was added to each well and was followed by 15 min of incubation to stain the cytoplasm. The cells were washed twice with PBS and filled with 200 μL of fresh medium. After staining the nuclei with 2 μL of Hoechst 33342 and quenching Cy3-fluorescence in the exterior of the cells by adding 2 μL of trypan blue solution (10 mg/mL), the cells were observed with an In Cell Analyzer 1000 (GE Healthcare, Buckinghamshire, U.K.) to evaluate cellular uptake of the polyplex micelles. The amount of cellular uptake of the polyplex micelles was quantified using the Cy3 fluorescence intensity per cell (intensity of Cy3 colocalized with calcein-stained cytoplasm divided by the number of cells).

2.13. Cell-Free Gene Expression Assay. Cell-free gene expression was evaluated using a TnT Quick Coupled Transcription/Translation System (Promega Co., Madison, WI). The polyplex micelles were prepared in the same manner as described previously, except for the use of luciferase T7 control DNA (T7-Luc) and were then incubated at 37 °C for 10 min. Solutions of naked pDNA or the polyplex micelles (each containing 1.33 μg of pDNA) were mixed with the cell-free system solution (TnT T7 Quick Master Mix) and incubated for 90 min at 37 °C according to the protocol provided by the manufacturer. Luciferase activity was evaluated using a Luciferase Assay System Kit (Promega Co., Madison, WI) and a Lumat LB 9507 luminometer (Berthold Technologies, Bad Wildbad, Germany).

2.14. In Vitro Transfection. Huh7 cells were seeded on 24-well culture plates (20000 cells/well) and incubated overnight with 400 μL of DMEM medium containing 10% FBS at 37 °C in a humidified atmosphere with 5% CO_2. After refreshing the medium, the polyplex micelle solutions were added to the cells (1.0 μg pDNA/well). The cells were incubated for 24 h and were incubated for an additional 24 h after the media was changed. Then, the cells were washed with PBS twice and lysed using 200 μL of lysate buffer. The luciferase activity of the cell lysate was evaluated using a Luciferase Assay System Kit (Promega Co., Madison, WI) and a Lumat LB 9507 luminometer (Berthold Technologies, Bad Wildbad, Germany).

3. RESULTS AND DISCUSSION

3.1. Preparation and Characterization of Block Copolymers and Polyplex Micelles. A triblock copolymer, PEtOx-*b*-PnPrOx-*b*-PLys, was synthesized through click conjugation between alkyne-PnPrOx-*b*-PEtOx and azide-PLys. Alkyne-PnPrOx-*b*-PEtOx was obtained by sequential polymerization of nPrOx and EtOx using propargyl *p*-toluenesulfonate as an initiator (Scheme 2i).[20,22,23] The resulting diblock copolymer had a M_w of 8030 for the PnPrOx segment and 9470 for the PEtOx segment, as determined by MALDI-TOF-MS analyses, with a fairly narrow molecular weight distribution of M_w/M_n = 1.01 (Table 1, Figure S1a,b). The composition of the diblock copolymer was consistently reconfirmed using ^{1}H NMR analyses (Figure S3a). Azide-PLys was synthesized by the ring-opening polymerization of NCA-*Nε*-(trifluoroacetyl)-L-lysine using 11-azido-3,6,9-trioxaundecan-1-amine as an initiator, followed by deprotection of the trifluoroacetyl group (Scheme 2ii). The DP was determined to be 46 from analysis of the ^{1}H NMR spectrum (Figure S3b). SEC measurements confirmed unimodal distribution of both the alkyne-PnPrOx-*b*-PEtOx and azide-PLys (Figure S2a,b). Subsequently, click conjugation between alkyne-PnPrOx-*b*-PEtOx and azide-PLys was carried out using the freeze−thaw technique using an excess of 2.5 equiv of the alkyne group compared to the azido group (Scheme 2iii). Note that the gradual freezing allows for local enrichment of the solute concentration, which could

Table 1. Characterization of block copolymers

	PEtOx M_w[a]	PnPrOx M_w[a]	POx M_w/M_n[a]	PLys DP[d]
Et9-Pr8-L	9470	8030	1.01[b]	46
Et18-L	17700		1.01[c]	46
Et10-L	10300		1.01[c]	46

[a]Determined from MALDI-TOF-MS spectra. [b]PEtOx-*b*-PnPrOx. [c]PEtOx. [d]Determined by ^{1}H NMR.

DOI: 10.1021/acs.biomac.5b01456
Biomacromolecules 2016, 17, 354−361

facilitate the reaction.[25] The SEC profile indicated the progress of quantitative click conjugation because no signals corresponding to azide-PLys were observed after the reaction (Figure S2c). Finally, the triblock copolymer of PEtOx-*b*-PnPrOx-*b*-PLys (denoted as Et9-Pr8-L) was isolated from the sample solution including excess alkyne-PnPrOx-*b*-PEtOx by precipitating the product against acetone. The narrow and unimodal profile of the prepared Et9-Pr8-L was confirmed by SEC (Figure S2d). Diblock copolymers of PEtOx and PLys without thermoresponsive properties were also prepared by click conjugation of alkyne-PEtOx and azide-PLys. Here, the DP of azide-PLys in the diblock copolymers was fixed to the same value with respect to the PLys segment in Et9-Pr8-L (DP_{PLys} = 46), whereas two lots of alkyne-PEtOx with different M_w of 10K and 18K were utilized for the reaction to obtain PEtOx-*b*-PLys denoted as Et10-L and Et18-L, respectively. Note that the total M_w of the PnPrOx and PEtOx segments in Et9-Pr8-L were comparable to those of the PEtOx segments in Et18-L, and the M_w of the PEtOx segments in Et9-Pr8-L was comparable to that of the PEtOx segment in Et10-L. Accordingly, both diblock copolymers can be regarded as controls for Et9-Pr8-L retaining no thermoresponsive units (Table 1).

The formation of the polyplex micelles was first examined for the complex prepared from the POx-based block copolymers at 4 °C (below the LCST of PnPrOx). The size determined by DLS measurements using a cumulant method, which measures the diameter of particles assuming spherical shape, was approximately 100 nm and a PDI of 0.22−0.29 for all the series of complexes prepared from the triblock copolymer and control diblock copolymers (Table 2). These values were comparable to previously studied polyplex micelles formed from poly(ethylene glycol) (PEG)-*b*-PLys with similar PLys DPs.[26,27] In addition, TEM observations revealed that these three POx-based complexes formed rod-shaped structures (Figure 2a, Figure S4c,g), which were typical structures of polyplex micelles.[26,27] Furthermore, the rod length distributions of these POx-based complexes measured from TEM images were consistent with the distributions predicted from a characteristic packaging scheme of pDNA in polyplex micelles, namely a quantized folding scheme (Figure S4a,d,h). These results were all consistent with features of the polyplex micelles that we have investigated. Therefore, it was reasonable to consider the newly synthesized POx-based block copolymers formed polyplex micelles with core−shell compartmentalized structures.

Table 2. Characterization of Polyplex Micelles

	cumulant diameter[a] (nm)	PDI[a]	average rod length[b] (nm)	
			4 °C	37 °C
Et9-Pr8-L	113	0.22	135 ± 56.8	90.0 ± 33.4
Et18-L	106	0.29	116 ± 39.8	119 ± 43.0
Et10-L	95	0.25	93.7 ± 28.5	93.7 ± 29.4

[a]Determined by DLS measurements at 15 °C. [b]Determined from TEM images of rod structures.

3.2. Thermoresponsivity of PnPrOx Segments within Polyplex Micelles. The thermoresponsivity of the PnPrOx segments installed in the polyplex micelles was examined by increasing the incubation temperature. First, ^{1}H NMR analysis was used to detect changes in the mobility of the PnPrOx segments by increasing the incubation temperature.[28] The signal intensities derived from the protons of the PnPrOx segment were expected to decrease in response to the LCST event due to a decrease in chain mobility. Indeed, a gradual decrease in signal intensity corresponding to the PnPrOx segment (δ = 0.83−0.98 ppm) occurred above 25 °C, suggesting the transition of the PnPrOx segments to dehydrated states (Figures 1a and S5a,b). Note that the intensity of the PEtOx segment (δ = 0.99−1.15) was not significantly affected by an increase in temperature, although it decreased slightly when the temperature exceeded 37 °C. Presumably, the transition of the PnPrOx segment upon LCST could influence the mobility of the PEtOx segments, especially those neighboring the PnPrOx blocks. Furthermore, the soluble−to-insoluble transition of the PnPrOx segments may have changed the morphologies of the polyplex micelles. In the structures of rod-shaped polyplex micelles, the compaction tendency of the polyplex core to reduce the developed unfavorable surface energy upon charge neutralization (the origin of DNA condensation) is hampered by steric repulsion derived from the hydrophilic shell.[27] In other words, the shell sustained the rod structure from becoming more compact. Regarding this balance, the rod length is expected to decrease in temperature above the LCST of PnPrOx because the collapse of the PnPrOx segments reduce steric repulsion of the shell as only the PEtOx segments remain in a hydrated state. Moreover, the collapsed PnPrOx segment is expected to develop unfavorable surface energy, which would also cause shortening of the rod lengths. DLS measurements of the polyplex micelles showed a significant drop in both size and PDI values when the temperature was increased from 20 to 25 °C. Then, a gradual decrease in size was observed at the temperature above 25 °C (Figure 1b). Furthermore, TEM observations revealed that the rod lengths of the polyplex micelles decreased from an average

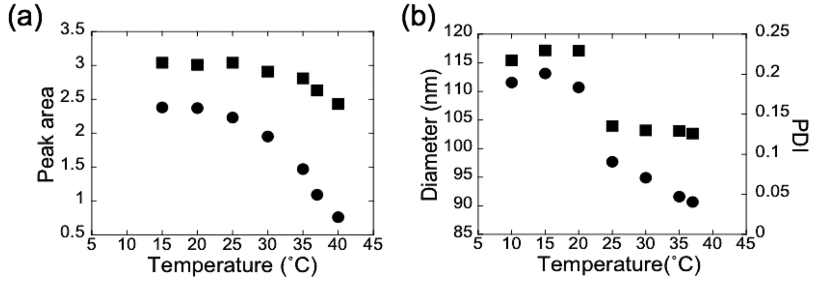

Figure 1. Evaluation of thermoresponsivity of the polyplex micelles prepared from Et9-Pr8-L. (a) Integrations of ^{1}H NMR signal areas derived from PnPrOx (●) and PEtOx (■) side chains within polyplex micelles with increased temperatures. (b) Cumulant diameter (●) and polydispersity index (PDI; ■) determined by DLS measurements with increased temperatures.

DOI: 10.1021/acs.biomac.5b01456
Biomacromolecules 2016, 17, 354−361

of 135 to 90.0 nm after incubation at 37 °C (Figure 2 and Table 2). Notably, after a thermal incubation at 37 °C, the

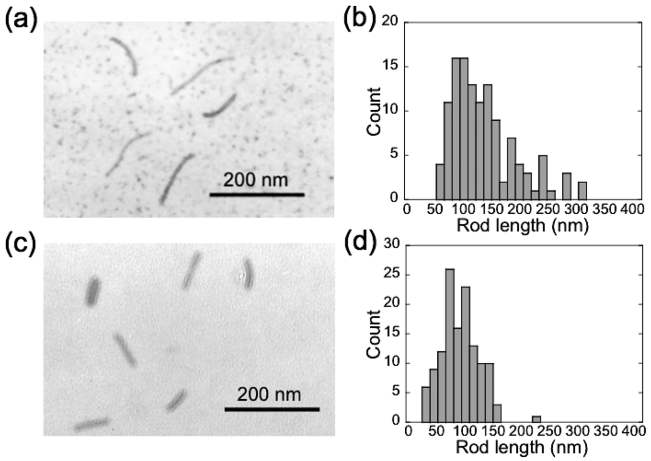

Figure 2. Representative TEM images and rod length evaluation of polyplex micelles of Et9-Pr8-L at 4 °C (a, b) and following incubation at 37 °C for 10 min (c, d).

average lengths of the shortened rods were comparable or even shorter than those of the polyplex micelles of the Et10-L diblock copolymer (93.7 nm), which did not contain a PnPrOx segment but had PEtOx segments with comparable molecular weights to the Et9-Pr8-L triblock copolymer. The reduced lengths of the rod-shaped polyplex micelles suggested that the PnPrOx segment transitioned to a collapsed state even within the polyplex micelles. It may be noticed that the ^{1}H NMR signal intensities did not show significant decreases between 20 to 25 °C (Figure 1a) although the sizes already demonstrated appreciable drops in this temperature range (Figure 1b). This observation suggests that the steric repulsion in the shell layer may have decreased prior to the apparent dehydration of the PnPrOx segments in the Et9-Pr8-L polyplex micelles, which induced the rod shortening. It is reported that the coil to globule transition upon heating of the thermoresponsive polymer, poly(*N*-isopropylacrylamide) (PNIPAM), in aqueous medium proceeds from a fully hydrated coil to an unperturbed coil (Θ state), followed by an abrupt change in the volume to a collapsed globule by dehydration.[29] Presumably, the significant drop in the rod size observed at the temperature (~20 °C) just below the apparent LCST of the PnPrOx segment may correspond to the transition from fully hydrated coils to unperturbed coils (Θ state) of PnPrOx, provoking a loss of balance in the interfacial free energy and steric repulsion to induce significant shortening of rod lengths. The transition from the hydrated coil to the Θ coil could not be detected in the ^{1}H NMR analysis because the segments were still in the aqueous phase even at Θ coil state without significant changes in relaxation times. The apparent decrease in the ^{1}H NMR signals with heating above 25 °C correlated well with the further gradual decreases in the rod lengths, which reflected the dehydration of the PnPrOx layer in the polyplex micelles. Furthermore, the invariable rod lengths of the control polyplex micelles prepared from the Et18-L and Et10-L diblock copolymers after the same thermal treatment (Figure S4, Table 2) further supported the occurrence of a coil-to-globule transition of PnPrOx within the polyplex micelles of Et9-Pr8-L in response to changes in temperature.

3.3. Estimation of the Coverage of Polyplex Micelle Core by Hydrophobized PnPrOx. The coverage of the polyplex core with collapsed PnPrOx segments was estimated to gain insight into the barrier properties of the hydrophobic layer. Coverage was evaluated by comparing the sum of the projection area of a collapsed PnPrOx segment for each chain ($A_{polymer} = m\pi R_{g(collapsed)}^2$) with the surface area of a polyplex micelle core ($A_{surface}$), where m and $R_{g(collapsed)}$ represent the number of PnPrOx segments in a polyplex micelle and the radius of gyration for a collapsed PnPrOx chain, respectively. Considering the charge stoichiometric nature of the complex prepared from cationic block copolymers and pDNA,[26,27] m was calculated as 282 using the following equation: 6477(bp) × 2/46 (= PLys DP). The $R_{g(collapsed)}$ of 1.53 nm for a PnPrOx segment with M_w 8030 was obtained from the description, $R_{g(collapsed)} = aN^{1/3}$, for a polymer in poor solvent,[30,31] using a monomer unit length (a = 0.37 nm) of poly(2-methyl-2-oxazoline)[32] taking a structural similarity to PnPrOx. Consequently, $A_{polymer}$ was calculated to be 2.07 × 10^3 nm^2. According to previously reported methods[27,33] (SI 6), $A_{surface}$ was obtained to be 5.47 × 10^3 nm^2 from analyses on the rod length distributions measured from TEM images. The coverage of the collapsed PnPrOx segments on the core was ultimately calculated to be 37.9% (=$A_{polymer}/A_{surface}$ × 100). Because this coverage was apparently insufficient to fully cover the core, the space between each collapsed PnPrOx segment was calculated under the assumption that each PnPrOx segment was arranged as a blob in a hexagonal lattice on the surface of the core (SI 7) to inspect the feasibility of the blocking properties. The calculation suggested that incursion of nucleases and GAGs was unlikely because the interspace was narrow enough to block them (1.67 nm, Figure S6). Note that the dimension of DNase I, a typical nuclease, is 4.5 × 4.0 × 3.5 nm[34] and that the persistence length of CS, the most abundant GAG, is reported to be 7−10 nm.[35] Therefore, the blocking properties could still be anticipated, even though the polyplex core may not be completely covered by the collapsed PnPrOx segment like a solid wall.

3.4. Effects of the Barrier Compartment on Improving the Stability of the Micelles. Following the estimates obtained above, the blocking property of the PnPrOx compartment as a hydrophobic palisade prepared by thermal treatment was examined against DNase I, the most abundant nuclease in the body. The control polyplex micelles, prepared from Et18-L diblock copolymers (no PnPrOx segment), displayed the remaining DNA as a smear pattern in the gel electrophoresis image under conditions that allowed naked DNA to receive complete digestion (Figure 3a). In contrast, clear, discrete DNA bands were observed in the electro-

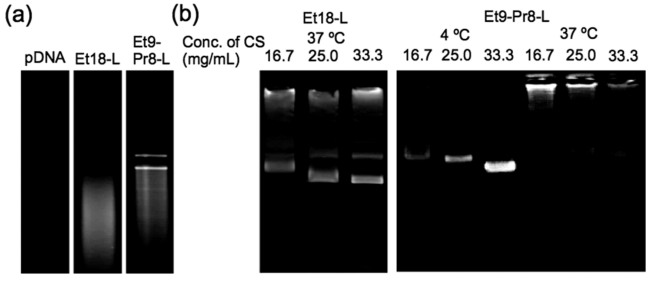

Figure 3. Tolerance of polyplex micelles against (a) DNase I and (b) CS attack determined by gel electrophoresis.

DOI: 10.1021/acs.biomac.5b01456
Biomacromolecules 2016, 17, 354−361

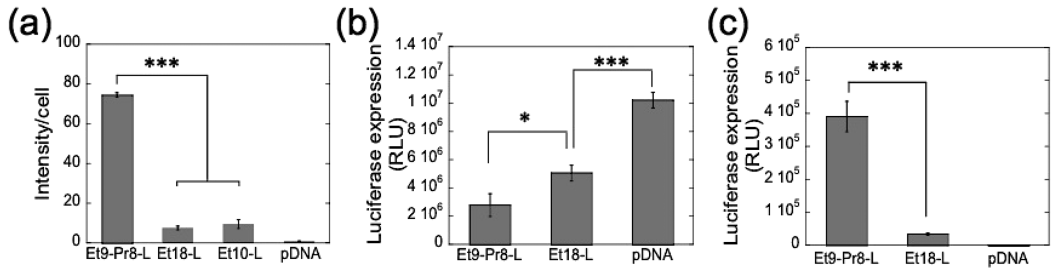

Figure 4. Effects of nPrOx barrier compartments on biological properties. (a) Cellular uptake (mean ± SEM, $n = 4$), (b) luciferase gene expression efficiency in a cell-free transcription/translation assay system (mean ± SEM, $n = 6$), and (c) luciferase gene expression against Huh7 cells (mean ± SEM, $n = 4$). The data were evaluated by a two-tailed Student's t test (*$p < 0.05$, ***$p < 0.001$).

phoretogram (Figure 3a) of the polyplex micelles of Et9-Pr8-L retaining the PnPrOx barrier compartment, verifying the significant blocking property of the PnPrOx palisades against DNase I.

The blocking property against polyion exchange was then evaluated using CS as a representative GAG in ECM and also on the cell surface.[14] While the control polyplex micelles of Et18-L without PnPrOx segments resulted in the release of encapsulated pDNA as a consequence of unpackaging, the polyplex micelles of Et9-Pr8-L retaining the PnPrOx compartment showed no DNA band corresponding to the release of pDNA (Figure 3b). Importantly, a demonstration at 4 °C showed that the polyplex micelles of the Et9-Pr8-L without forming hydrophobic palisades resulted in the release of pDNA (Figure 3b), similar to the control polyplex micelles without PnPrOx segments. These results further verified the significant blocking properties of the collapsed PnPrOx segments and their behavior as hydrophobic barrier compartments against CS.

3.5. Cellular Transfection by Polyplex Micelles with Barrier Compartments. The presence of PnPrOx barrier layers was expected to increase the cellular uptake efficiency of the polyplex micelles by improving their stability. An evaluation on the cellular uptake of Huh7 cells showed that the polyplex micelles of Et9-Pr8-L with barrier compartments exhibited significantly higher uptake efficiencies compared to those of the control polyplex micelles of Et18-L without PnPrOx segments (Figure 4a). It should be noted that possible contributions of micelles with the reduced thickness of the hydrophilic shell layer and the reduced rod length caused by thermal treatment to the cellular uptake may be negligible because Et10-L polyplex micelles with comparable PEtOx shell compartments and rod lengths to the thermally treated Et9-Pr8-L polyplex micelles revealed a substantially lower extent of cellular uptake. Therefore, the promotion of cellular uptake efficiency was most likely due to the improved stability of the polyplex micelles with barrier compartments.

There may be a concern in overstabilization of the polyplex micelles with hydrophobic PnPrOx layer, hampering the ability to release loaded pDNA properly at the interior of transfected cells. Accordingly, gene expression was evaluated using a cell-free transcription/translation system composed of cell lysates to avoid the effects of cellular uptake and endosome escapability. The Et9-Pr8-L polyplex micelles exhibited gene expression, although their efficiencies decreased to half of that of the control Et18-L polyplex micelles without hydrophobic middle compartments (Figure 4b), suggesting that the Et9-Pr8-L polyplex micelles permitted transcription even with the barrier compartment. Note that the spontaneous dissociation of polyplex micelles in solution is unlikely because previous investigations on PLys-based polyplex micelles presented sufficient stability within physiological NaCl concentrations[26] and serum.[27] Thus, transcription likely occurred within the polyplex micelles. Previous studies showed that polyplex micelles actually allow for transcription.[26,36] Presumably, PLys segments bound on DNA had enough mobility to permit transcription, clearing the way for the transcription machinery to slide along the DNA chain. This mobility may have permitted transcription even with the collapsed PnPrOx blobs linked to PLys, although the efficiency would decrease. Nevertheless, as gene expression proceeds, it may be still possible to anticipate a promotion in cellular transfection as long as the benefits gained from improved stability can compensate for the diminished capability for gene expression. Actually, this may be likely because the Et9-Pr8-L polyplex micelles exhibited 10 times greater cellular uptake efficiencies than the Et18-L polyplex micelles (Figure 4a), while the former polyplex micelles were half as efficient in gene expression as the latter polyplex micelles (Figure 4b). Subsequent transfection efficiencies evaluated against Huh7 cells showed that the Et9-Pr8-L polyplex micelles exhibited significantly increased gene expression efficiencies that were 10× greater than those of the Et18-L polyplex micelles (Figure 4c), which was consistent with our expectations. Importantly, the series of POx-based polyplex micelles presented no remarkable cytotoxicity (Figure S7), fulfilling issues of safety. Consequently, the promoted gene transfection efficiencies demonstrated the great utility of triblock copolymer-mediated polyplex micelles with hydrophobic palisades assigned in the middle compartments, which were employed using a smart "thermal switch" concept and the intriguing properties of a thermoresponsive polymer.

4. CONCLUSIONS

With the aim of improving the stability of polyplex micelles to promote their gene transduction efficiency, we designed POx-based triblock copolymers with a thermoresponsive unit to form a protective hydrophobic barrier compartment that was spatially positioned between the pDNA core compartment and the hydrophilic outer shell of the polyplex micelles. The thermoswitchable property of PnPrOx was utilized to prepare a hydrophilic middle layer after packaging the regularly folded pDNA in the core of the polyplex micelles under conditions below LCST of the PnPrOx segments, thereby stabilizing the polyplex micelles with uniform sizes and well-compartmentalized structures. The formation of a hydrophobic protective palisade was consistently confirmed through ^{1}H NMR, DLS, and TEM techniques. Eventually, the prepared polyplex micelles provided remarkable improvements in stability against both DNase I and CS attacks, and demonstrated promotion in

DOI: 10.1021/acs.biomac.5b01456
Biomacromolecules 2016, 17, 354−361

transfection with increased cellular uptake. Although the calculations suggest that the density of the collapsed PnPrOx segments in the middle layer may not be high enough to fully cover the pDNA core, we still observed the enhanced transfection efficiencies of Et9-Pr8-L polyplex micelle compared to the micelle without PnPrOx layer (Et18-L polyplex micelle). This indicates the high feasibility of the proposed smart polyplex micelle prepared from thermoswitchable POx-based triblock copolymers as nonviral gene vectors used in harsh biological environments.

■ ASSOCIATED CONTENT

Supporting Information

The Supporting Information is available free of charge on the ACS Publications website at DOI: 10.1021/acs.biomac.5b01456.

Characterization of synthesized polymers by size exclusion chromatography (SEC), ^{1}H NMR and MALDI-TOF MS, evaluation of control polyplex micelles by TEM, ^{1}H NMR spectrum of polyplex micelles of Et9-Pr8-L taken at 15 and 40 °C, estimation of the core surface area of thermally treated polyplex micelles of Et9-Pr8-L and the interspace between each collapsed PnPrOx chain on the core, and evaluation of Huh7 cells viability after transfection by polyplex micelles (PDF).

■ AUTHOR INFORMATION

Corresponding Authors

*E-mail: osada@bmw.t.u-tokyo.ac.jp.
*E-mail: kataoka@bmw.t.u-tokyo.ac.jp.

Notes

The authors declare no competing financial interest.

■ ACKNOWLEDGMENTS

This work was financially supported by Center of Innovation (COI) program and "Precursory Research for Embryonic Science and Technology" (PRESTO) in "Molecular Technology and Creation of New Functions" from the Japan Science and Technology Corporation (JST), and the Japan Society for the Promotion of Science (JSPS) through Specially Promoted Research Program, and Core to Core Program for Advanced Research Networks. The authors are grateful to Dr. Satoshi Fukuda from the University of Tokyo Hospital for his valuable support in conducting TEM.

■ REFERENCES

(1) Katayose, S.; Kataoka, K. *Bioconjugate Chem.* **1997**, *8*, 702−707.
(2) Kakizawa, Y.; Kataoka, K. *Adv. Drug Delivery Rev.* **2002**, *54*, 203−222.
(3) Miyata, K.; Nishiyama, N.; Kataoka, K. *Chem. Soc. Rev.* **2012**, *41*, 2562−2574.
(4) Lachelt, U.; Wagner, E. *Chem. Rev.* **2015**, *115*, 11043−11078.
(5) Merdan, T.; Kunath, K.; Petersen, H.; Bakowsky, U.; Voigt, K. H.; Kopecek, J.; Kissel, T. *Bioconjugate Chem.* **2005**, *16*, 785−792.
(6) Mintzer, M. A.; Simanek, E. E. *Chem. Rev.* **2009**, *109*, 259−302.
(7) Wu, Y.; Wang, M.; Sprouse, D.; Smith, A. E.; Reineke, T. M. *Biomacromolecules* **2014**, *15*, 1716−1726.
(8) Fukushima, S.; Miyata, K.; Nishiyama, N.; Kanayama, N.; Yamasaki, Y.; Kataoka, K. *J. Am. Chem. Soc.* **2005**, *127*, 2810−2811.
(9) Wei, H.; Volpatti, L. R.; Seller, D. L.; Maris, D. O.; Andrews, I. W.; Hemphill, A. S.; Cham, L. W.; Chu, D. S. H.; Horner, P. J.; Pun, S. H. *Angew. Chem., Int. Ed.* **2013**, *52*, 5377−5381.
(10) Nomoto, T.; Fukushima, S.; Kumagai, M.; Machitani, K.; Arnida; Matsumoto, Y.; Oba, M.; Miyata, K.; Osada, K.; Nishiyama, N.; Kataoka, K. *Nat. Commun.* **2014**, *5*, 3545.
(11) Dirisala, A.; Osada, K.; Chen, Q.; Tockary, T. A.; Machitani, K.; Osawa, S.; Liu, X.; Ishii, T.; Miyata, K.; Oba, M.; Uchida, S.; Itaka, K.; Kataoka, K. *Biomaterials* **2014**, *35*, 5359−5368.
(12) Novo, L.; van Gaal, E. V.; Mastrobattista, E.; van Nostrum, C. F.; Hennink, W. E. *J. Controlled Release* **2013**, *169*, 246−256.
(13) Tumova, S.; Woods, A.; Couchman, J. R. *Int. J. Biochem. Cell Biol.* **2000**, *32*, 269−288.
(14) Malavaki, C.; Mizumoto, S.; Karamanos, N.; Sugahara, K. *Connect. Tissue Res.* **2008**, *49*, 133−139.
(15) Burke, R. S.; Pun, S. H. *Bioconjugate Chem.* **2008**, *19*, 693−704.
(16) Belting, M.; Petersson, P. *J. Biol. Chem.* **1999**, *274*, 19375−19382.
(17) Zuckerman, J. E.; Choi, C. H. J.; Han, H.; Davis, M. E. *Proc. Natl. Acad. Sci. U. S. A.* **2012**, *109*, 3137−3142.
(18) Sedlacek, O.; Monnery, B. D.; Filippov, S. K.; Hoogenboom, R.; Hruby, M. *Macromol. Rapid Commun.* **2012**, *33*, 1648−1662.
(19) Hoogenboom, R.; Thijs, H. M. L.; Jochems, M. J. H. C.; van Lankvelt, B. M.; Fijten, M. W. M.; Schubert, U. S. *Chem. Commun.* **2008**, 5758−5760.
(20) Park, J. S.; Kataoka, K. *Macromolecules* **2007**, *40*, 3599−3609.
(21) Hernandez, J. R.; Klok, H. A. *J. Polym. Sci., Part A: Polym. Chem.* **2003**, *41*, 1167−1187.
(22) Fijten, M. W. M.; Haensch, C.; Lankvelt, B. M.; Hoogenboom, R.; Schubert, U. S. *Macromol. Chem. Phys.* **2008**, *209*, 1887−1895.
(23) Kempe, K.; Baumgaertel, A.; Hoogenboom, R.; Schubert, U. S. *J. Polym. Sci., Part A: Polym. Chem.* **2010**, *48*, 5100−5108.
(24) Kolb, H. C.; Finn, M. G.; Sharpless, K. B. *Angew. Chem., Int. Ed.* **2001**, *40*, 2004−2021.
(25) Takemoto, H.; Miyata, K.; Ishii, T.; Hattori, S.; Osawa, S.; Nishiyama, N.; Kataoka, K. *Bioconjugate Chem.* **2012**, *23*, 1503−1506.
(26) Osada, K.; Shiotani, T.; Tockary, T. A.; Kobayashi, D.; Oshima, H.; Ikeda, S.; Itaka, K.; Kataoka, K. *Biomaterials* **2012**, *33*, 325−332.
(27) Tockary, T. A.; Osada, K.; Chen, Q.; Machitani, K.; Dirisala, A.; Uchida, S.; Nomoto, T.; Toh, K.; Matsumoto, Y.; Itaka, K.; Nitta, K.; Nagayama, K.; Kazunori, K. *Macromolecules* **2013**, *46*, 6585−6592.
(28) Kourilova, H.; Spevacek, J.; Hanykova, L. *Polym. Bull.* **2013**, *70*, 221−235.
(29) Wu, C.; Wang, X. *Phys. Rev. Lett.* **1998**, *80*, 4092−4094.
(30) Wang, R.; Wang, Z. G. *Macromolecules* **2014**, *47*, 4094−4102.
(31) Schild, H. G. *Prog. Polym. Sci.* **1992**, *17*, 163−249.
(32) Ivanova, R.; Komenda, T.; Bonné, T. B.; Lüdtke, K.; Mortensen, K.; Pranzas, P. K.; Jordan, R.; Papadakis, C. M. *Macromol. Chem. Phys.* **2008**, *209*, 2248−2258.
(33) Osada, K.; Oshima, H.; Kobayashi, D.; Doi, M.; Enoki, M.; Yamasaki, Y.; Kataoka, K. *J. Am. Chem. Soc.* **2010**, *132*, 12343−12348.
(34) Suck, D.; Oefner, C.; Kabschl, W. *EMBO J.* **1984**, *3*, 2423−2430.
(35) Bathe, M.; Rutledge, G. C.; Grodzinsky, A. J.; Tidorz, B. *Biophys. J.* **2005**, *88*, 3870−3887.
(36) Li, Y.; Osada, K.; Chen, Q.; Tockary, T. A.; Dirisala, A.; Takeda, K. M.; Uchida, S.; Nagata, K.; Itaka, K.; Kataoka, K. *Biomacromolecules* **2015**, *16*, 2664−2671.

DOI: 10.1021/acs.biomac.5b01456
Biomacromolecules 2016, 17, 354−361